Original Article

Photoluminescence characteristics of SiO_2-GeO_2-R_2O (R: Na, K, Rb, and Cs) glasses

Taro Asahi (Faculty of Fundamental Science, National Institute of Technology (KOSEN), Niihama College, t.asahi@niihama-nct.ac.jp, Japan)
Noriyuki Wada (Department of Materials Science and Engineering, KOSEN, Suzuka College, n.wada@szuka-nct.ac.jp, Japan)
Susumu Nakayama (Department of Applied Chemistry and Biotechnology, KOSEN, Niihama College, s.nakayama@niihama-nct.ac.jp, Japan)

Abstract

This study fabricates $50SiO_2{\cdot}50GeO_2$ and $50SiO_2{\cdot}(50\text{-}x)GeO_2{\cdot}xR_2O$ (R: Na, K, Rb, and Cs, x = 5–40) glasses using the conventional melt-quenching method. Their photoluminescence characteristics were investigated by measuring their emission and excitation spectra. In the case of the $50SiO_2{\cdot}50GeO_2$ glass, a sharp and significant emission band attributed to the Ge^{2+} center appeared prominently at a central wavelength of 395 nm, corresponding to an excitation band at 250 nm. However, the emission spectra of $50SiO_2{\cdot}(50\text{-}x)GeO_2{\cdot}xR_2O$ glasses revealed distinct emission bands around 480 and 540 nm, which differ from the 395 nm emission band typically associated with the Ge^{2+} center. These emission bands indicated coordination of the Ge^{2+} center with alkali ions. The basicity of alkali oxide, which is linked to its ability to provide O^{2-} ions, influenced the coordination of the Ge^{2+} center with alkali ions in the glasses, resulting in a decrease in the amount of coordination. Consequently, the intensity of the emission bands varied depending on the quantity and type of alkali components present.

Key words

network modifier oxide, non-bridging oxygen, oxygen vacancy, alkali ions, basicity

1. Introduction

Photoluminescent glass is typically produced by incorporating an activation agent, such as rare earth and transition elements, into the glass matrix during the melting process (Guo et al., 2016; Hwang et al., 2022; Mawlud et al., 2024). Various defects exist in the germanate glass matrix, including the germanium electron trapped center, germanium E′ center, neutral oxygen monovacancy, Ge^{2+} center (natural oxygen divacancy), self-trapped hole center, non-bridging oxygen hole center (Ge-$O^{\cdot}$), and peroxy radical. Notably, the Ge^{2+} center exhibits dual emission bands centered at 300 and 395 nm, corresponding to excitation bands at 250 and 330 nm (Skuja, 1989; Nishii, 1998). Studies have shown that the emission and excitation bands ascribed to the Ge^{2+} center species shift with the addition of alkali and alkaline earth oxides (Trukhin, 2009; Teng et al, 2010). Furthermore, the intensity of the emission band attributed to the Ge^{2+} center at 399 nm decreases with increasing amounts of alkali and alkaline earth oxides in germanate glasses (Wada, 2006). Apart from the Ge^{2+} center, various defects in oxide glass can lead to optical absorption, distinct from the effects of the activation agent (Skuja et al., 2000; Trukhin and Golant, 2007; Trukhin, 2009). Additionally, adjusting the absorption energy towards the activation agent can potentially develop high-power fluorescent glass.

A previous study demonstrated that the near-white luminescence phenomenon was observed in glasses containing $50SiO_2{\cdot}(50\text{-}x)GeO_2{\cdot}xNa_2O$ upon the addition of alkali oxide to $50SiO_2{\cdot}50GeO_2$ glasses (Nakayama et al., 2017; Asahi et al., 2017). In the present study, we synthesized $50SiO_2{\cdot}(50\text{-}x)GeO_2{\cdot}xR_2O$ glasses (R: Na, K, Rb, and Cs, x = 5–40) and investigated the relationship between fluorescence properties and glass composition through their emission and excitation spectra.

2. Experimental

Germanosilicate and alkali germanosilicate glasses were prepared using the conventional melt-quenching method. The reagents, GeO_2 (Kojundo Chemical Laboratory Co., 99.99 %), SiO_2 (Fujifilm Wako Pure Chemical Co., 99.9 %), and R_2CO_3 (R: Na, K, Rb, and Cs: Fujifilm Wako Pure Chemical Co., Special Grade), were utilized as starting materials. They were weighed to the desired glass batch composition and mixed. The resulting powder mixture was placed into a Pt–13%Rh crucible with a lid and melted in an electric furnace at 1500 °C in an air atmosphere. After melting for 1 h, the crucible was removed and cooled by blowing air with a hairdryer to solidify the glass melt. The obtained samples were ground using a zirconium mortar and subjected to X-ray diffraction (XRD) measurements (Rigaku Co., MiniFlex II) to confirm vitrification. X-ray photoelectron spectroscopy (XPS) measurements of the Gd3*d* electronic state were conducted using a PHI5000 VersaProb system (Ulvac-phi Inc.) equipped with a monochromatized Al-Kα X-ray source ($h\nu$ = 1486.6 eV). A spot diameter of 100 μm was considered for the analysis, and the resulting binding energies were calibrated by setting the C 1s peak (C–C bond) to 284.8 eV. Finally, the emission and excitation spectra were recorded using a fluorescence spectrometer (Shimadzu Co., RF-6000) employing a 150-W ozone-free Xenon lamp at a scan rate of 500 nm min^{-1} and step size of 0.1 nm.

3. Results and discussion

3.1 XRD analysis

The XRD spectra of the samples prepared for $50SiO_2{\cdot}(50\text{-}x)GeO_2{\cdot}xNa_2O$ (x = 5–40) and $50SiO_2{\cdot}20GeO_2{\cdot}30R_2O$ (R: Na, K, Rb, and Cs) are depicted in Figure 1. Small diffraction peaks corresponding to the $Na_2Si_2O_5$ (ICDD No. 23-529) and Na_2SiO_3 (ICDD No. 16-818) phases were observed in the $50SiO_2{\cdot}(50\text{-}x)GeO_2{\cdot}xNa_2O$ (x = 5–40) series XRD pattern for x = 40. For x = 5–35, the $50SiO_2{\cdot}(50\text{-}x)GeO_2{\cdot}xNa_2O$ (x = 5–40) and $50SiO_2{\cdot}20GeO_2{\cdot}30R_2O$ (R: Na, K, Rb, and Cs) series revealed only a halo-like XRD pattern, which confirms that these samples did undergo vitrification. All the prepared $50SiO_2{\cdot}(50\text{-}x)GeO_2{\cdot}xNa_2O$ (x = 5–40) and $50SiO_2{\cdot}20GeO_2{\cdot}30R_2O$ (R: Na, K, Rb, and Cs) samples appeared transparent. The $50SiO_2{\cdot}20GeO_2{\cdot}30Li_2O$ sample did not vitrify using the preparation method reported herein; instead, it underwent crystallization.

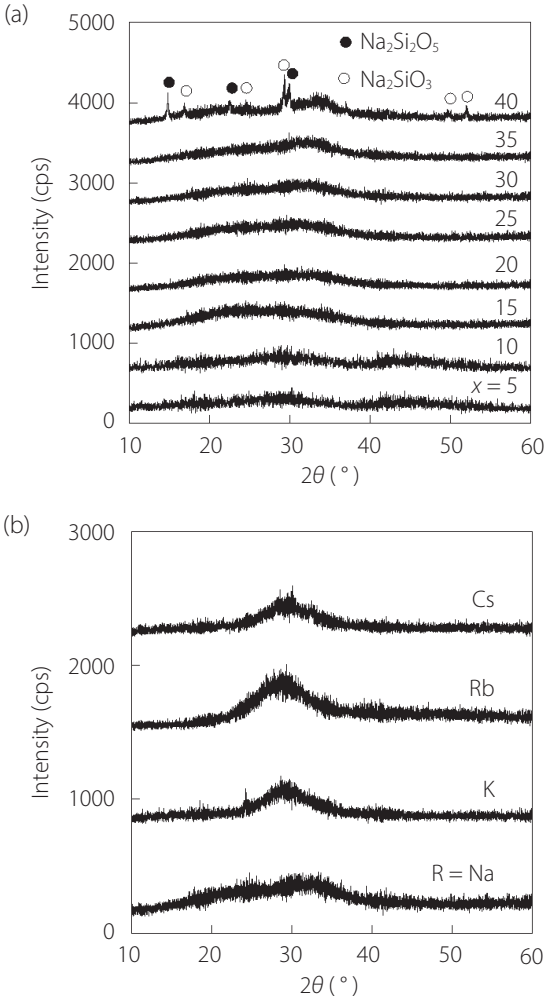

Figure 1: XRD patterns of (a) $50SiO_2{\cdot}(50\text{-}x)GeO_2{\cdot}xNa_2O$ (x = 5–40) and (b) $50SiO_2{\cdot}20GeO_2{\cdot}30R_2O$ (R: Na, K, Rb, and Cs) samples

Note: Closed and open circles denote $Na_2Si_2O_5$ and Na_2SiO_3 phases, respectively.

3.2 XPS analysis

The Gd3*d* XPS spectra of the $50SiO_2{\cdot}20GeO_2{\cdot}30Na_2O$ and $50SiO_2{\cdot}20GeO_2{\cdot}30K_2O$ glasses are shown in Figure 2 (a) and (b), respectively. Peaks corresponding to the Ge 3*d* state were detected at 30.96 and 33.22 eV for the $50SiO_2{\cdot}20GeO_2{\cdot}30Na_2O$ glass, as determined by peak deconvolution (Asahi et al., 2017). Moreover, peaks corresponding to the Ge 3*d* state were detected at 31.37 and 32.73 eV for the $50SiO_2{\cdot}20GeO_2{\cdot}30K_2O$ glass. Wang et al. reported Ge–O peaks corresponding to the chemical species $Ge_3{\equiv}Ge{-}O$ (Ge^{1+}), $Ge_2{=}Ge{=}O_2$ (Ge^{2+}), $Ge{-}Ge{\equiv}O_3$ (Ge^{3+}), and $O{-}Ge{\equiv}O_3$ (Ge^{4+}) at 30.88, 31.78, 32.69, and 33.57 eV, respectively, for $(SiO_2)_{50}(GeO_2)_{50}$ (Wang et al., 1998); this indicates that the Ge atoms in the $50SiO_2{\cdot}20GeO_2{\cdot}30Na_2O$ and $50SiO_2{\cdot}20GeO_2{\cdot}30K_2O$ glasses exhibit two distinct valence states (Ge^{2+} and Ge^{4+}). In our study, these two valence states were observed in the $50SiO_2{\cdot}20GeO_2{\cdot}30Na_2O$ and $50SiO_2{\cdot}20GeO_2{\cdot}30K_2O$ glasses at ratios of 13.67/86.33 and 15.42/84.58, respectively, supporting the aforementioned results obtained by Wang et al.

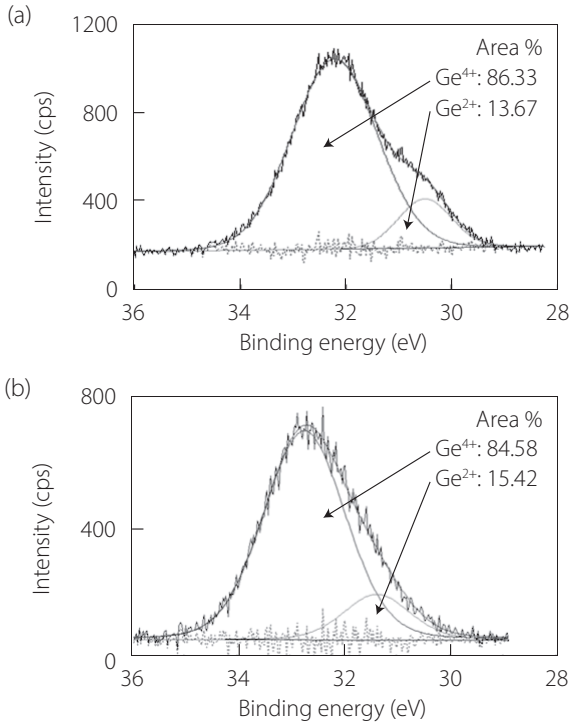

Figure 2: Ge 3*d* XPS spectra of (a) $50SiO_2{\cdot}20GeO_2{\cdot}30Na_2O$ and (b) $50SiO_2{\cdot}20GeO_2{\cdot}30K_2O$ glasses

3.3 Photoluminescence characteristics

The emission and excitation spectra, along with the excitation–emission matrices, of $50SiO_2{\cdot}50GeO_2$ and $50SiO_2{\cdot}20GeO_2{\cdot}30Na_2O$ glasses are shown in Figure 3. In the case of $50SiO_2{\cdot}50GeO_2$, the emission peak occurs at a narrow range of 400 nm, corresponding to excitation at a near short-wavelength ultraviolet region, resulting in a blue emission phenomenon. Conversely, for the $50SiO_2{\cdot}20GeO_2{\cdot}30Na_2O$

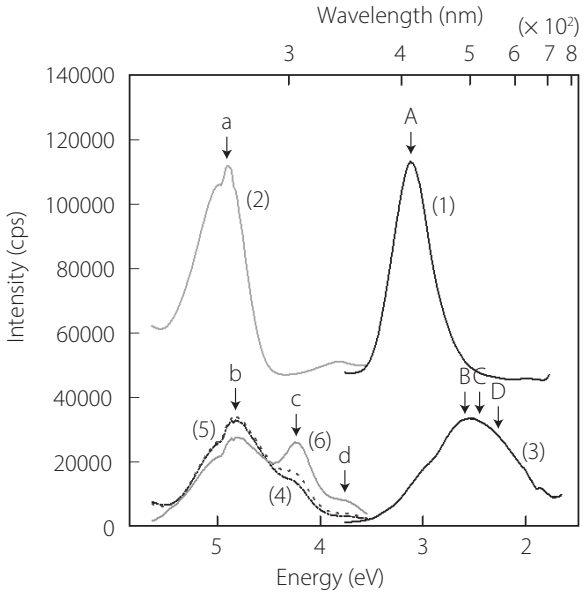

Figure 3: Emission and excitation spectra of $50SiO_2{\cdot}50GeO_2$ and $50SiO_2{\cdot}20GeO_2{\cdot}30Na_2O$ glasses

Note: (1) λ_{em} =253 nm, (2) λ_{em} =397 nm, (3) λ_{em} =258 nm, (4) λ_{em} =475 nm, (5) λ_{em} =487 nm, and (6) λ_{em} =549 nm.

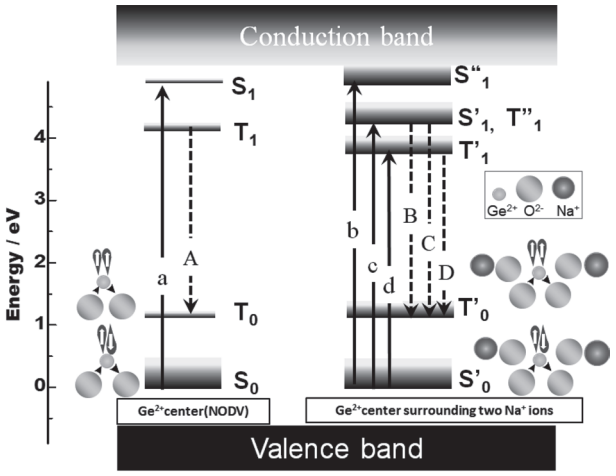

Figure 4: Schematic of the energy level of (a) $50SiO_2{\cdot}50GeO_2$ and (b) $50SiO_2{\cdot}20GeO_2{\cdot}30Na_2O$ glasses

glass, new emission peaks emerged in the range of 500 to 600 nm, corresponding to the near 300 nm excitation range, leading to a near-white emission phenomenon. The fluorescent color coordinates for $50SiO_2{\cdot}50GeO_2$ and $50SiO_2{\cdot}20GeO_2{\cdot}30Na_2O$ were (0.172, 0.059) and (0.283, 0.333), respectively. The substitution of Na_2O for GeO_2 in the $50SiO_2{\cdot}50GeO_2$ series was found to alter the fluorescence characteristics.

Emission (corresponding to (1) in Figure 3) and excitation (corresponding to (2) in Figure 3) spectra of $50SiO_2{\cdot}50GeO_2$ glass included the emission band *A* and excitation band *a* at 397 and 253 nm, respectively. These two bands are attributed to the Ge^{2+} center, a defect in the germanate glass. However, in the $50SiO_2{\cdot}20GeO_2{\cdot}30Na_2O$ glass, the emission band *B* and *C* appeared at positions 475 and 487 nm without reducing the intensity of the emission band *A*. Additionally, a new emission band *D* emerged at 549 nm. Consequently, emission bands *B*, *C*, and *D* contributed to the broadening of the emission spectra (corresponding to (3) in Figure 3). In the excitation spectra (corresponding to (4), (5), and (6) in Figure 3) for the ascribed emission bands *B*, *C*, and *D*, excitation bands at 255, 292, and 330 nm appeared as band *b*, *c*, and *d*, respectively. Thus, in glass samples containing alkali oxide, it was observed that emission bands *B*, *C*, and *D* appeared instead of the emission band *A* ascribed to the Ge^{2+} center. Additionally, excitation bands *b*, *c*, and *d* appeared instead of the excitation band *a*. These results indicate that new emission and excitation bands observed in spectra (3), (4), (5), and (6) are attributed to Ge^{2+} center coordinated Na^+ ions.

Figure 4 illustrates the energy diagram for the Ge^{2+} center inferred from the emission and excitation spectra shown in Figure 3. Both the emission band at 300 nm and the excitation band at 330 nm were initially unlikely to appear due to forbidden singlet-to-triplet transitions for the Ge^{2+} center, in the $50SiO_2{\cdot}50GeO_2$ glass samples. However, in the $50SiO_2{\cdot}20GeO_2{\cdot}30Na_2O$ glass samples, the forbidden transitions from singlet to triplet were allowed through the coordination with Na^+ ions, resulting in the observation of excitation bands *b*, *c*, and *d* instead of the excitation band a. The coordination of the Ge^{2+} centers with Na^+ ions could potentially lead to the splitting of energy levels within a distorted local glass structure, forming multiple energy levels based on the position and orientation of alkali ions in the glass samples. Therefore, it is proposed that the appearance of emission bands *B*, *C*, and *D* reflect transitions between the T_0' energy level and the T_1' and T_1'' ones.

Figure 5 shows emission spectra in the sample of $50SiO_2{\cdot}(50\text{-}x)GeO_2{\cdot}xNa_2O$ series. For *x* up to 30, both emission bands *B* and *C* exhibited increased intensity with higher alkali contents. The maximum intensity of emission bands *B* and *C* occurs at $x = 30$. Conversely, for *x* values exceeding 30, the intensity of bands *B* and *C* decreased with higher alkali oxide contents, albeit at different rates. Furthermore, emission bands *B* and *C* shifted toward longer wavelengths. These changes are attributed to the distortion of the local structure of the Ge^{2+} center and the gradual disappearance of Ge^{2+} centers with increasing alkali content. The Na_2O component, functioning as a glass network modifier with high basicity, introduces oxide ions (O^{2-}) into the glass melt. This addition of oxide ions leads to the formation of non-bridging oxygen, altering the local glass structure from tight to loose, ultimately resulting in the disappearance of Ge^{2+} centers in the glass samples.

The emission spectra of the $50SiO_2{\cdot}20GeO_2{\cdot}30R_2O$ series depicted in Figure 6 show that the spectrum of sodium series (R:

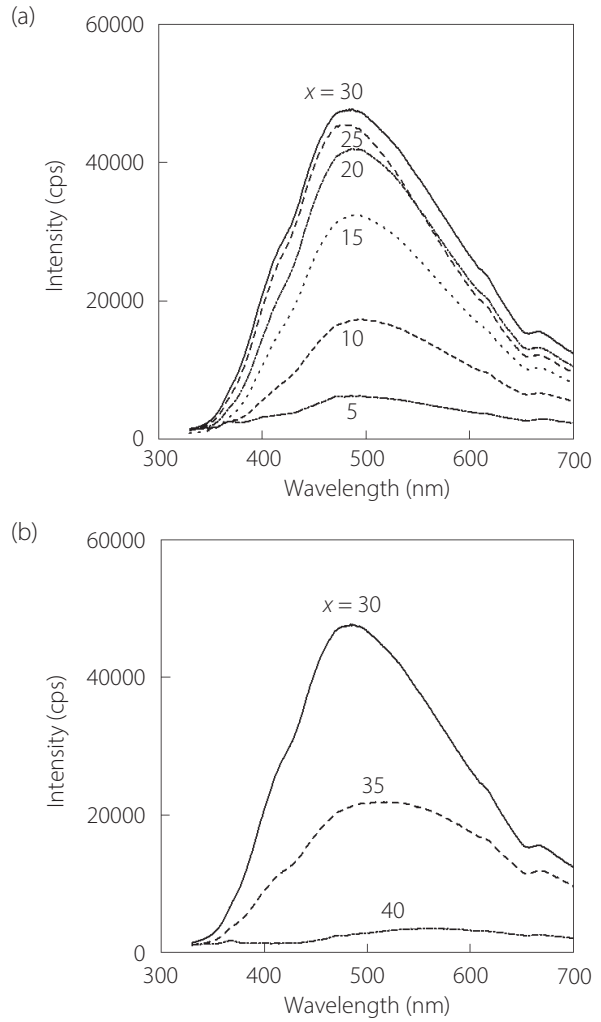

Figure 5: Emission spectra of 50 SiO_2·(50-*x*) GeO_2·*x*Na_2O ((a): *x* = 5, 10, 15, 20, and 25, (b): *x* = 30, 35, and 40) glasses excited at 250 nm

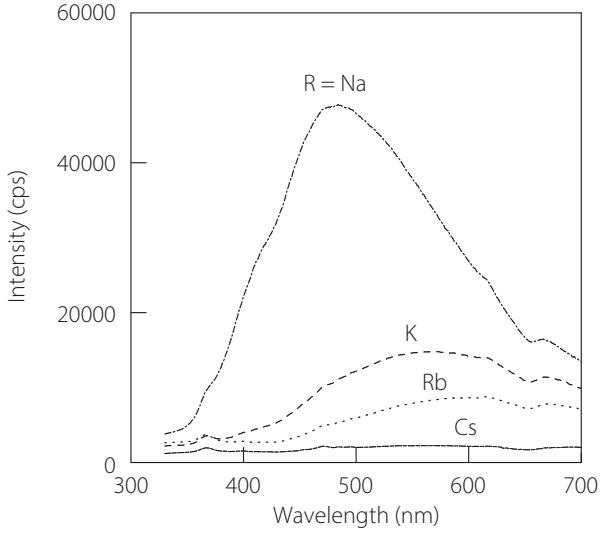

Figure 6: Emission spectra of 50SiO_2·20GeO_2·30R_2O (R: Na, K, Rb, and Cs) glasses excited at 250 nm

Na) exhibits the maximum intensity. The fluorescent color coordinates for 50SiO_2·20GeO_2·30R_2O (R: Na, K, Rb, and Cs) were (0.283, 0.333), (0.369, 0.40), (0.392, 0.403), and (0.346, 0.364), respectively. Emission bands *B* and *C* decrease in the following sequence: Na → K → Rb → Cs. The basicity of alkali oxides follows a similar trend: Na_2O → K_2O → Rb_2O → Cs_2O. Alkali and alkaline earth oxides, acting as glass network modifiers with high basicity and large ionic radius, significantly influence the structure of Ge^{2+} centers by providing oxide ions into the glass melt. Consequently, the distortion and dispersion of Ge^{2+} centers in the glass increase accordingly. Moreover, the emission bands *B* and *C*, attributed to Ge^{2+} centers coordinated with alkali ions, vary based on the type and quantity of alkali species.

4. Conclusions

In this study, we investigated the photoluminescence characteristics of 50SiO_2·(50-*x*)GeO_2·*x*R_2O glass in comparison to 50SiO_2·50GeO_2 glass. In the emission spectrum corresponding to the addition of alkali oxide to 50SiO_2·50GeO_2 glass, in addition to the emission band due to the Ge^{2+} center, new emission bands and excitation bands due to the Ge^{2+} center coordinated with alkali ions are observed. The intensity of these novel emission bands varies with the alkali content, reaching its maximum value at *x* = 30. Additionally, the intensity of emission bands associated with Ge^{2+} centers coordinated with alkali ions decreases with increasing alkali ion radius. The relationship between the intensity of emission bands and glass compositions is linked to the basicity of alkali oxide. As alkali oxide functions as a glass network modifier, the addition of highly basic alkali oxide provides ample oxide ions to the Ge^{2+} centers in the glass melt. Consequently, the amount of Ge^{2+} centers coordinated with alkali ions decreases in the glass samples, leading to a reduction in the intensity of the corresponding emission bands.

Acknowledgement

We would like to thank Editage (www.editage.jp) for English language editing.

References

Asahi, T., Omura, Y., Wada, N., and Nakayama, S. (2017). Photoluminescence of sodium germanosilicate glass synthesized by melting mixture of SiO_2, GeO_2, and Na_2CO_3. *Optik*, Vol. 149, pp. 423-429.

Guo, H., Wang, Y., Gong, Y., Yin, H., Mo, Z.. Tang, Y., and Chi, L. (2016). Optical band gap and photoluminescence in heavily Tb^{3+} doped GeO_2-B_2O_3-SiO_2-Ga_2O_3 magneto-optical glasses. *Journal of Alloys and Compounds*, Vol. 686, pp. 635-640.

Hwang, Y. S., Aryal, P., Kim, H. J., Ntarisa, A. V., Saha, S., Kim, C., Kothan, S., and Kaewkhao, J. (2022). Mn^{2+} doping inside

glass substrate utilizing metal ion beam implantation technique. *Optik*, Vol. 262, 169270.

Mawlud, S. Q., Ahmed, A. A., and Aziz, S. M. B. (2024). Enhancement of luminescence properties of Sm^{3+} doped tellurite glass embedded with gold nanoparticles: Heat treatment. *Results in Optics*, Vol. 14, 100587.

Nakayama, S., Asahi, T., Omura, Y., Tsuji, H., and Okubo, N. (2017). Effect of various additives on fluorescent intensity of GeO_2·SiO_2 phosphor. *Optik*, Vol. 142, pp. 54-60.

Nishii, J. (1998). Permanent index changes in Ge-SiO_2 glasses by excimer laser irradiation. *Materials Science and Engineering: B*, Vol. 54, pp. 1–10.

Skuja, L. N. (1989). Photoluminescence of intrinsie defects in glassy GeO_2. twofold coordinated ge and nonbridging oxygen. *Physica Status Solidi (a)*, Vol. 114, pp. 731-737.

Skuja, L. N., Hosono, H., Mizuguchi, M., Güttler, B., Silin, A., and Makishima, A. (2000). Site-selective study of the 1.8 eV luminescence band in glassy GeO_2. *Journal of Luminescence*, Vol. 87-89, pp. 699-701.

Teng, Y., Zhuang, Y., Lin, G., Zhou, J., Zhu, B., and Qiu, J. (2010). Luminescence properties of reduced SrO-Al_2O_3-GeO_2 glasses. *Journal of Alloys and Compounds*, Vol. 494, pp. 378-381.

Trukhin, A. N. and Golant, K. M. (2007). Absorption and luminescence in amorphous silica synthesized by low-pressure plasmachemical technology. *Journal of Non-Crystalline Solids*, Vol. 353, pp. 530-536.

Trukhin, A. N. (2009). Luminescence of polymorph crystalline and glassy SiO_2, GeO_2: A short review. *Journal of Non-Crystalline Solids*, Vol. 355, pp. 1013-1019.

Wada, N., Ichinotani, M., and Kojima, K. (2006). Glass composition dependence of luminescence due to Ge^{2+} center in germanate glasses. *Journal of Non-Crystalline Solids*, Vol. 352, pp. 2657-2661.

Wang, P. W., Qi, Y., and Henderson, D. O. (1998). Oxygen bonding in GeO_2 glass. *Journal of Non-Crystalline Solids*, Vol. 224, pp. 31-35.

Received: April 17, 2025
Accepted: May 26, 2025
Published: June 30, 2025

https://doi.org/10.11425/sst.14.31